Book of Tutorials and Abstracts

European Microbeam Analysis Society

EMAS 2023

17th

EUROPEAN WORKSHOP

on

MODERN DEVELOPMENTS AND APPLICATIONS IN MICROBEAM ANALYSIS

7 to 11 May 2023
at the
Jagiellonian University, Auditorium Maximum
Krakow, Poland

Under the auspices of the Rector of the
Jagiellonian University, Krakow, Poland
Organised in collaboration with the
Institute of Metallurgy and Materials Science of
the Polish Academy of Sciences, Krakow, Poland

EMAS
European Microbeam Analysis Society eV
www.microbeamanalysis.eu/

This volume is published by:
European Microbeam Analysis Society eV (EMAS)
EMAS Secretariat
c/o Eidgenössische Technische Hochschule, Institut für Geochemie und Petrologie
Clausiusstrasse 25
8092 Zürich
Switzerland

ISBN 978 90 8227 6961
NUR code: 972 – Materials Science

LOCAL, ABSOLUTE RESIDUAL STRAIN MEASUREMENTS USING COMBINED RING-CORE MILLING AND CROSS-CORRELATION EBSD IN AN SEM

Stefan Zaefferer and H. Khanchandani

Max-Planck Institut für Eisenforschung GmbH, Diffraction and Microscopy Group
Max-Planck Strasse 1, 40237 Düsseldorf, Germany
e-mail: s.zaefferer@mpie.de

Stefan Zaefferer received his PhD at the Technical University of Clausthal in Germany. Then he spend three years as a researcher at the University Paris XII in Paris, France, and two years at Kyoto University, Japan. Since 2000 he heads the group "Microscopy and Diffraction" at the Max-Planck-Institute for Iron Research in Düsseldorf (Germany) and is lecturer for materials characterisation at RWTH Aachen University. He also teaches regularly at Vienna University. At all his research positions her was involved with the development and application of techniques for individual orientation determination and lattice defect characterisation, first by TEM techniques and then, most prominently, by SEM techniques. Besides development of diffraction techniques his research interests are the mechanisms of microstructure formation in metals and other materials, including deformation, re-crystallisation and phase transformation. Stefan Zaefferer is author or co-author of about 150 journal papers. He is co-author together with Olaf Engler and Valerie Randle of the 3rd edition of the book "Introduction to texture analysis", which will be published in 2023.

1. ABSTRACT

The present paper describes a new method to measure local residual stresses at an absolute level including first, second and third kind residual stresses. The method is based on the combination of cross-correlation EBSD analysis with ring-core milling to create strain free reference positions in every grain. The advantages of the new technique with respect to the two individual techniques are discussed. Preliminary measurements on a deformed stainless steel sample are very promising and indicate that the method works as expected. We propose more systematic investigations and improvements to the method which will be employed soon.

2. INTRODUCTION TO THE MEASUREMENT OF ELASTIC STRAINS IN THE SEM

2.1. Cross-correlation electron backscatter diffraction

Electron backscatter diffraction (EBSD) has become probably the most powerful tools for quantitative materialography. It allows – at least in the limits of spatial and angular resolution – quantitative characterisation of all aspects of microstructures, including grains (morphology and texture), phases (secondary phases, precipitations), grain and phase boundaries (misorientations and planes), dislocations (densities and types, at least for geometrically necessary dislocations, GND), and other features like cracks or shear bands or other plastic strain fields. An important component of microstructures are residual stresses that form during many materials processes and influence many materials structural or functional properties. Residual stresses are tensorial values that consist of 3 normal and 3 shear stresses. With cross-correlation (CC) analysis of EBSD patterns the EBSD technique is also able to measure 3rd kind residual stresses with a spatial resolution as good as that of EBSD in general (between 50 and 500 nm, depending on the investigated material) and an elastic strain resolution of about $\Delta\varepsilon/\varepsilon = 10^{-4}$ [1]. The measurement is performed by a high accuracy geometric comparison of EBSD patterns with a very similar reference pattern from within the same grain. Note, that in order to reach a sufficient accuracy the geometry of EBSD patterns has to be measured to about a 1/20 of a pixel. The measured residual stress is, thus, always described relative to a stress level within the same grain. It is important to note that residual stresses are categorised into 1st to 3rd kind as it is indicated in Fig. 1. First kind are macroscopic residual stresses, usually caused by mechanical or thermomechanical processes applied to the material. Second kind residual stresses are changing from crystal to crystal. They are due to the different elasto-plastic behaviour of differently oriented crystals. The third kind stresses, finally, are caused by the accommodation of different elastic and plastic deformation behaviour of neighbouring crystals and due to any heterogeneous deformation inside of grains. At every position in a material, all 3 kinds of residual stresses add together component-wise and build-up the total stress (or strain) level.

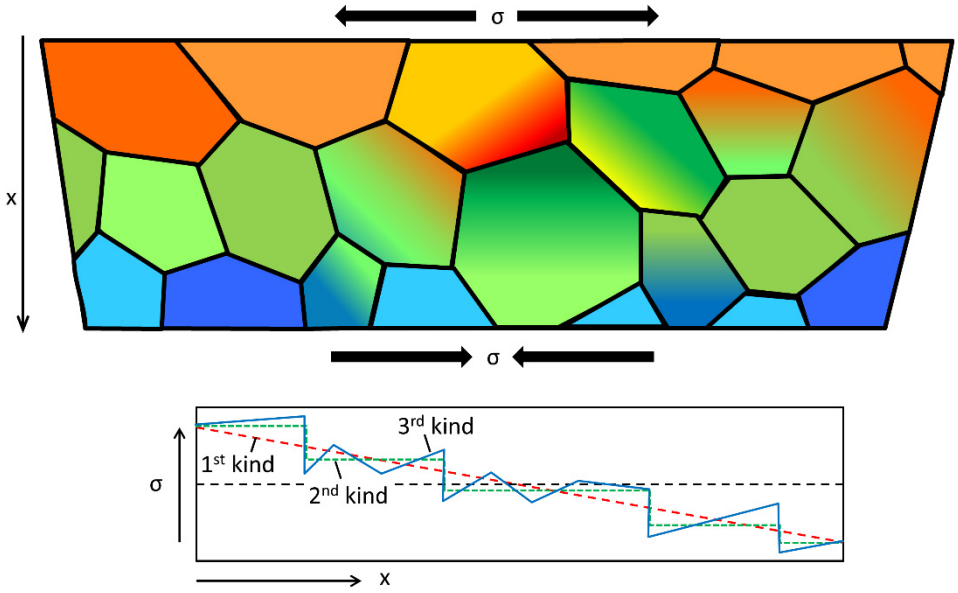

Figure 1. Schematic display of residual stresses in a polycrystalline material under a bending strain load. Colours indicate the stress level (red high positive, blue low negative). The top surface is under tensile stresses, the bottom under compressive stresses (1st kind stresses). Individual grains have different stress levels because of their different crystal orientations (2nd kind stresses). Inside of the grains different accommodation stresses appear with different neighbours (3rd kind stresses).

From EBSD only the 3rd kind stresses are measured and this leaves, of course, the picture incomplete. It is not possible to determine whether the measured stresses refer to a total stress level of 0 or any negative or positive bias. In the past is has been tried to overcome this shortcoming by various approaches. One is a high-resolution 3D Hough transform (3D HT), which measures the hyperbolic shape of the Kikuchi lines in the EBSD patterns [2]. This approach is, in principle, similar to the measurement of residual stresses from Kossel patterns [3], with the unfortunate difference that the curvature of Kikuchi lines in EBSD patterns is much smaller than that of Kossel cones and its detection therefore less accurate. Note here that Kossel patterns are currently still the most accurate approach to measure absolute residual stresses on a several-micron resolution level. In order to reach a sufficient level of accuracy with a 3D HT on EBSD patterns would require determining the projection centre of the pattern with very high accuracy, which is currently not possible.

Another approach that has been proposed is the use of simulated diffraction patterns using a highly realistic dynamic electron diffraction model [4]. Also this approach fails because of the missing projection centre accuracy. Approaches have also been made to fit the simulated diffraction pattern to the measured one and then iteratively change crystal orientation (3 parameters) and projection centre (3 parameters) until a minimum is found [5]. As far as the author knows also this approach, so far, has not lead to a satisfactory absolute stress determination. Here the reasons are manifold: First a 6-parameter fitting procedure at

sub-pixel-resolution requires a lot of calculations and the correct minimum is rather shallow. The probably most important shortcoming is, however, that the simulated patterns do not take into account the appearance of excess and deficiency lines that are due to the anisotropic illumination of the crystal in an EBSD experiment. Simulated patterns only show dark Kikuchi lines while real ones show, depending on the orientation, dark or bright Kikuchi lines. Figure 2 shows an example of a simulated and a measured diffraction pattern of the [111] pole in aluminium. The simulated diffraction pattern shows perfectly symmetric band profiles while this is not the case for the experimental one, as indicated by the arrows.

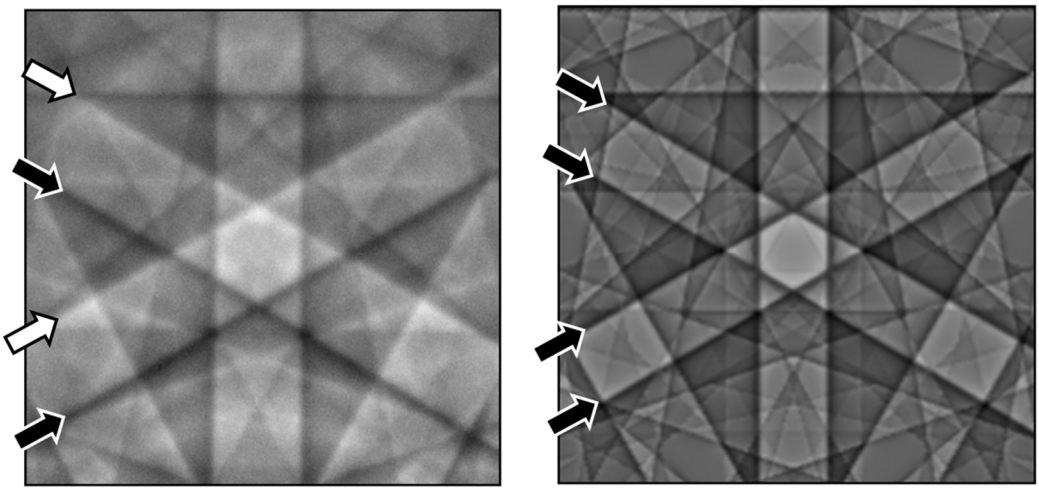

Figure 2. Experimental (left) and simulated (right) EBSD pattern of aluminium. The experimental pattern shows excess (bright) and deficiency (dark) Kikuchi lines, while the simulated one shows only dark lines. Simulations performed with Esprit-S (Bruker, Aimo Winkelmann).

2.2. Ring-core milling (RCM)

A completely different approach to the determination of residual stresses is the measurement of the relaxation strain when a specimen with residual stresses is cut free. This is the basis of the borehole method, which is usually used for the measurement of macroscopic residual stresses. Note that the method is destructive, in contrast to the diffraction techniques. Korsunsky *et al.* [6] and later Sebastiani *et al.* [7] have transferred this method to the microscopic level by using a ring-milling approach with a focussed ion beam (FIB) instrument to free-cut a cylinder-shaped area at a few-micrometre diameter. The principle is displayed in Fig. 3. Before the ring-core milling, a microscopic pattern is applied to the area of interest (e.g., by FIB deposition of platinum dots). An SE image of this pattern is recorded and saved. During the ring-core milling the pattern is regularly recorded again. Using digital image correlation (DIC) the recorded patterns are compared to the original one to determine the stress relaxation process. The measured strains are then interpreted as residual stresses before the milling. This approach has been taken up by the group of the current author to measure the elastic distortion

within a martensitic steel microstructure [8] and on additive manufactured high entropy alloy [9]. One result of the former work is reproduced in Fig. 4. The method has the advantage to determine the absolute elastic strain in the material and does not require any reference point. The main disadvantages, however, are that the method is rather tedious, it is of limited resolution (we used ring diameters in the order of 5 µm), it is not a mapping technique but only good for collection of scattered individual data, and that it only measures plane strains and not the full strain tensor. Furthermore, the DIC process is very sensitive to any kind of recording artefact, e.g., distortion of the scan fields by various reasons. Also, the ion beam can lead to modifications of the DIC pattern which then influences the results.

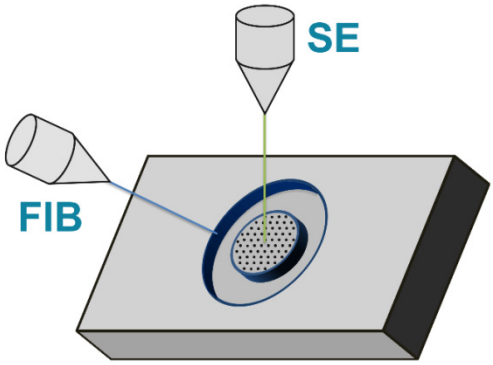

Figure 3. Geometrical set-up of ring-core milling. The focussed ion beam (FIB) is used to mill the ring and deposit a surface pattern. Secondary electrons (SE) are used to observe the pattern during milling.

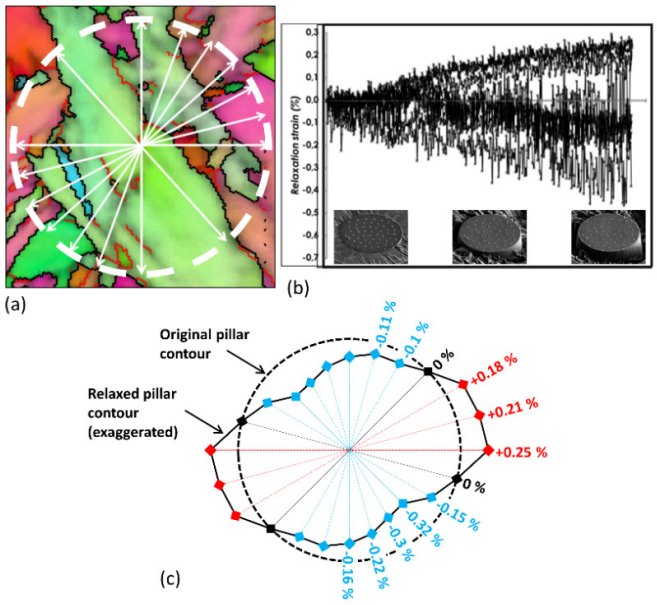

Figure 4. Results of ring-core milling on a martensitic steel. a) Microstructure before the milling, overlaid with the ring position and some of the directions in which the relaxation stresses are measured by digital image correlation. b) Relaxation graph displaying the evolution of strain in different directions with increasing milling depth. The x-axis displays the number of milling processes from 0 to 120. c) Final relaxation stresses for different directions.

2.3. A new technique: Combining CC EBSD and ring-core milling

We now propose a new technique, which takes advantage of both techniques, ring-core milling and CC EBSD and, at the same time circumvents many of the problems related to each of the individual techniques. The basis of the technique is the assumption that the interior of a milled ring is free of residual stresses if the ring has been milled deep enough and its diameter is small enough. In this case, an EBSD pattern obtained from the interior of the ring can be used as absolute reference pattern for all further patterns within the grain. In this way, a number of significant advantages are obtained: First, the total residual stress value is measured and all advantages of the CC EBSD method can be used, except for the area immediately around the ring where also the stresses outside of the ring is relaxed. The smaller the area is, the smaller is the ring diameter. CC EBSD is a true mapping technique, which allows measurement of all relevant areas inside of the grain, particularly including the areas next to neighbouring grains. Next, the relaxation itself of the ring-core does not need to be observed, it needs only to be made sure that the ring-core is relaxed. This eliminates a lot of difficulties related to proper and artefact-free scanning and does not require any surface pattern. On the other side, the technique can only be applied to grains that are several times larger in diameter than the ring diameter, and, of course, every grain requires one ring-core to be milled, if possible in the centre of the grain. This requires significantly more work than simple CC EBSD measurements.

3. EXPERIMENTAL DETAILS

As test material a 316L stainless steel sample was selected. The CC EBSD measurements were carried out on a Zeiss XB1540 FIB-SEM with field emission gun. This SEM is equipped with an EDAX/TSL EBSD system with a Hikari camera with 480 × 480 pixels pattern resolution. EBSD maps were measured at 20 kV acceleration voltage with a step size of 0.2 µm and a full-frame exposure of 1 second per pattern. Next, the sample was tilted to 54° such that the sample surface can be observed perpendicular with the focussed ion beam. From the previously measured orientation map, positions inside of each grain were selected for the milling of ring-cores of 1 µm diameter. For the milling a Ga^+-ion beam accelerated in a 30 kV electric field was selected. A beam current of 500 pA was used which offered the best compromise of good focus and rapid milling. Altogether 6 rings with a diameter of 1 µm and a depth of about 2 µm were milled into the sample, as shown in Fig. 5. Each ring took about 1 minute to be milled. During the milling process care was taken to irradiate the area surrounding the ring as little as possible in order not to destroy the lattice. After milling was accomplished, a second CC EBSD map of the same area was measured using the same parameters as before.

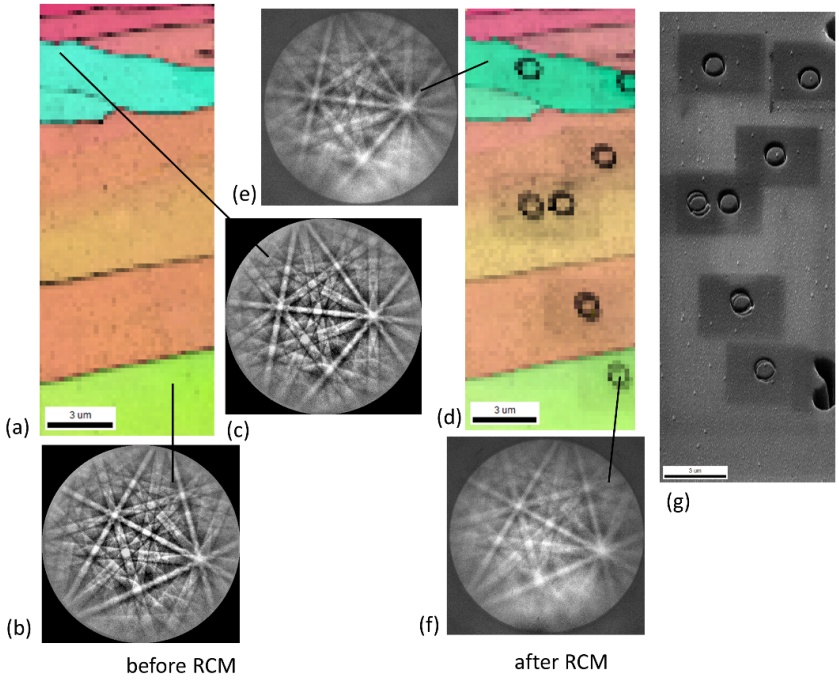

Figure 5. EBSD maps before and after ring-core milling. a) Inverse pole figure (ND) map of the sampled area before RCM overlaid with pattern quality grey value. b and c) Two typical diffraction patterns from a). d) As a) after RCM. e) EBSD pattern of an area close to a milled ring. f) EBSD pattern from an area in a ring-core. g) SE image of ring-cores on the sample surface.

4. RESULTS AND DISCUSSION

Our investigations are still at a preliminary state. Nevertheless, we have been able to create a number of systematic ring-core millings and CCEBSD measurements. The EBSD maps before and after the RCM process are displayed in Fig. 5 as inverse pole figure (IPF) maps overlaid with the pattern quality as grey value. The small circles found on the RCM structure correspond to the milled rings. They are more clearly visible in the SE image Fig. 5g. The RCM structure shows faint dark windows around the individual rings, which indicate the area where the FIB scanned (even only shortly) to find the correct milling place and to focus. The EBSD patterns that are displayed in Figs. 5e and 5f show that the pattern quality reduces quite dramatically in these areas and also, in the middle of the ring-core. This is, of course, highly undesired because the patterns from these areas will serve as reference patterns for the rest of the grain. It is thus essential to keep the milling and FIB observation time as short as possible. The allowed dose needs to be determined by future systematic studies. Re-deposition of milled material in the centre of the ring deteriorates the pattern quality. This is becoming more important with increasing width of the ring and decreasing diameter. It appears that the here selected ring diameter of 1 µm and ring width of 200 nm is the smallest value. Figure 6 displays a comparison of the total pattern quality of the area before RCM and after RCM. It is very obvious that the pattern quality is reduced in the material after RCM. In fact, the extent of reduction surprises

and is probably not only due to the milling process (which effects only a small part of the whole map) but potentially due to the previous orientation mapping which deposits a thin carbon contamination film on the sample. In a future approach, this contamination film will be removed by applying 5 minutes of *in-situ* plasma cleaning of the sample.

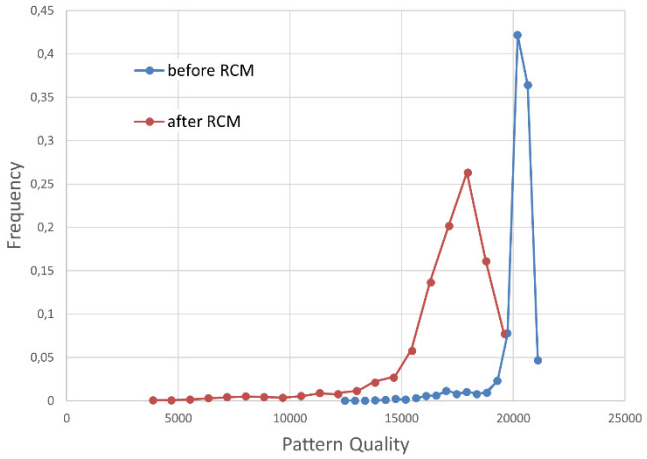

Figure 6. Comparison of diffraction pattern quality before and after ring-core milling. Large numbers indicate high quality patterns.

While the pattern quality is reduced in the surrounding of the milled area, there is no additional deformation or orientation change introduced as this is visible in the grain reference orientation (GROD) and local orientation spread maps displayed in Fig. 7. The maps show that the rings themselves are wrongly indexed but the ring-cores are unaffected. The maps also show that the ring-core is only about 3 × 3 pixels of 0.2 µm step size wide, which appears the minimum acceptable value for later pattern correlation. An inner ring diameter of 1.5 µm will be the better choice.

Figure 8, finally, displays first results of cross correlation measurements. Figure 8a shows the position of the individual grains. For each of which a separate cross correlation analysis is performed. For the cross-correlation results the top row maps display the quality of the cross-correlation. Here again the effect of FIB or electron beam irradiation is quite obvious. The bottom row maps are the von-Mises stress maps, calculated from the individual elastic stress components, which themselves are calculated from the individual elastic strains. Von-Mises stress are selected as representative value for all individual stress tensor components. Note that the total strain level of maximum 5 GPa is clearly too high to be true. This is a known artefact of the technique, which can be significantly reduced by applying a so-called remapping analysis [10]. For the Figs. 8b and 8c, the cross-correlation has been calculated based on reference points with high pattern quality and positioned explicitly outside of ring-cores. The reference points for the individual grains are marked by small black pixels. This analysis is performed to show that the ring-core milling does not affect the local elastic strain distribution. In an ideal case,

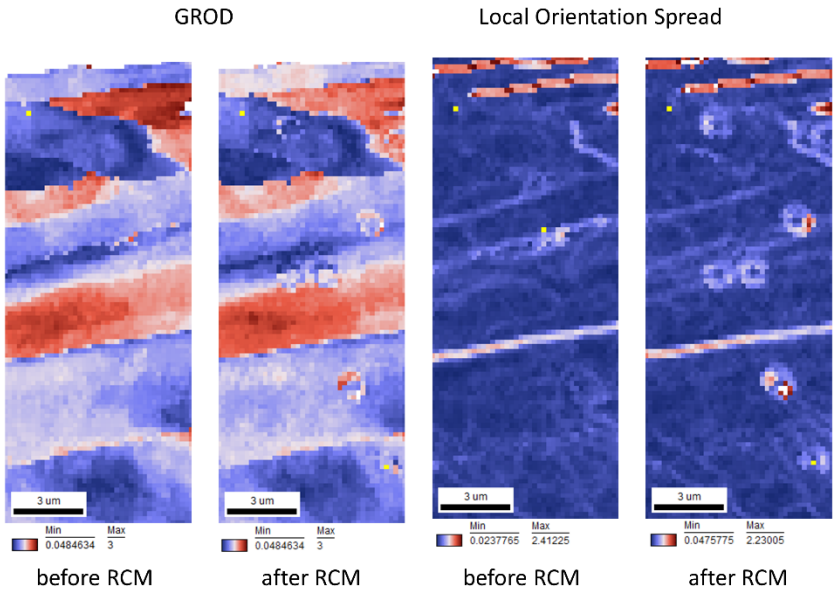

Figure 7. Grain reference orientation deviation (GROD) map and local orientation spread maps before and after ring-core milling (RCM). The GROD map sensitively displays orientation changes the local orientation spread displays the occurrence of local plastic strain. For both maps, the ring-cores do not show any particularities.

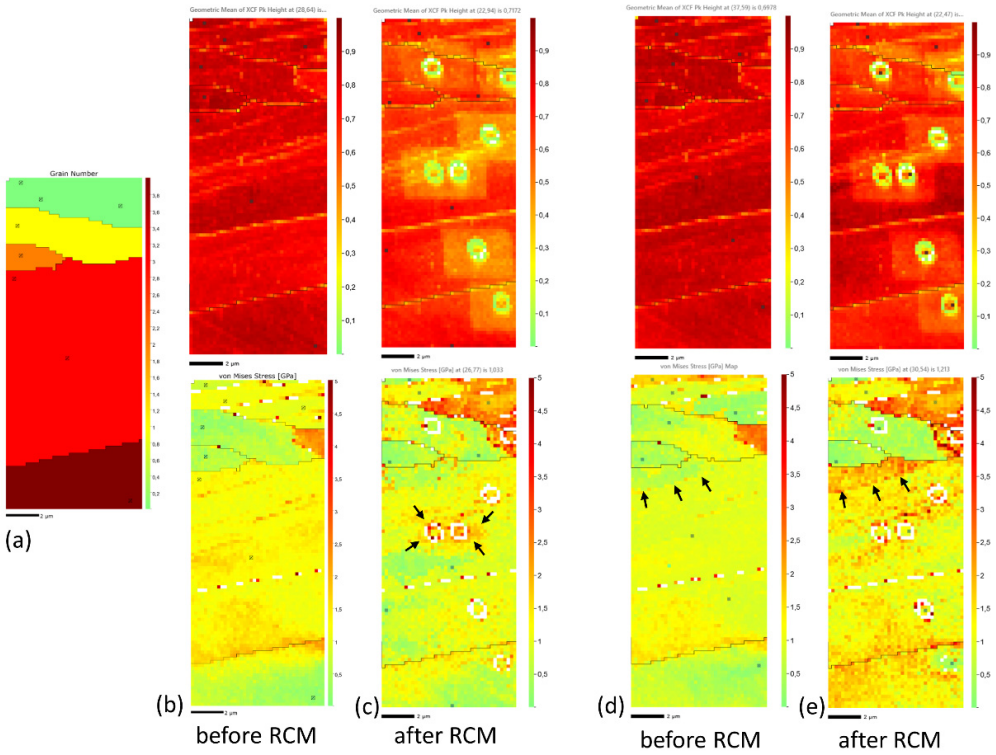

Figure 8. Results of cross-correlation EBSD analysis before and after RCM with different reference points. The top row images display the cross-correlation quality, the bottom row the von-Mises stresses. a) Grain map of the investigated area. b and c) With reference points of highest pattern quality outside of the RCM areas. d and e) With reference points inside of the ring-cores.

we expect that the maps in Figs. 8b and 8c are identical, with exception of the areas around the rings. A comparison of Figs. 8b with 8c shows that the milled rings lead to small strain effects in their surroundings which extend over about 1 ring diameter. One particularly obvious area is marked by black arrows in Fig. 8c. It is likely that a strain relaxation occurs not only inside of the ring but also in the direct surrounding, which may be the origin of the observed effects. Besides this, both maps are not perfectly identical. One reason for this may be the general degradation of the diffraction pattern quality of the RCM area (see Fig. 5) due to the previous EBSD observation, which contaminated the area with a thin carbon film. For future experiments plasma cleaning before and after ring-core milling appears essential. Also, the reference points are not exactly identical, which may lead to deviations because the material is deformed. For the data in Figs. 8d and 8e, the-cross correlation reference points have been selected such that they are inside of the ring-cores, as it is the idea of the new method. It is very obvious that the RCM in Fig. 8e leads to a significant change of the stress level of individual grains compared to Fig. 8d, see e.g., the grain marked by black arrows in the figures. Also the grain at the bottom of the map shows a significant change of stress level. In the present case, unfortunately, it is not known how high are the 1st or 2nd kind residual stresses in the sample, thus the analysis remains here incomplete for the moment. Nevertheless, the approach shows a clear effect without creating large additional artefacts. More reliable measurements on material with known long-range residual stresses will be carried out shortly.

5. CONCLUSIONS

The local measurement of residual stresses using cross correlation (CC) EBSD so far suffers from the fact that long-range stress fields of first and second kind cannot be measured. Here we propose a new technique, which combines ring-core milling (RCM) with CC EBSD to obtain the full elastic strain tensor of every grain. In the present case, RCM does not require any strain measurement by digital correlation but is just carried out to create a strain-free reference point inside of every grain. It was found that sample irradiation by both, the electron beam and the ion beam must be kept as short as possible to avoid pattern degradation. Also rings smaller than 1 µm in diameter do not appear reasonable because of pattern quality degradation in its centre. An optimum size seems to be 1.5 µm diameter. From literature, it is assumed that the depth of milling should be about as large as the diameter of the ring. First results suggest a strong effect on the measured stress level if a stress-free reference point within the ring-core is used as reference, which has, however, to be confirmed by further systematic measurements.

6. REFERENCES

[1] Wilkinson A J, Meaden G and Dingley D J 2006 *Ultramicroscopy* **106** 307-313
[2] Maurice C and Fortunier R 2008 *J. Microscopy* **230** 520-529

[3] Langer E and Däbritz S 2010 *IOP Conf. Ser.: Mater. Sci. Eng.* **7** 012015
[4] Adams B L, Fullwood D T, Basinger J A and Hardin T 2012 *Mater. Sci. Forum* **702** 11-17
[5] Winkelmann A, Jablon B M, Tong V S, Trager-Cowan C and Mingard K P 2020 *J. Microscopy* **277** 79-92
[6] Lunt A J and Korsunsky A M 2015 *Surf. Coatings Technol.* **283** 373-388
[7] Korsunsky A M, Sebastiani M and Bemporad E 2010 *Surf. Coatings Technol.* **205** 2393-2403
[8] Archie F, Mughal M Z, Sebastiani M, Bemporad E and Zaefferer S 2018 *Acta Materialia* **150** 327-338
[9] Sun Z, Tan X, Wang C, Descoins M, Mangelinck D, Tor S B, Jägle E A, Zaefferer S and Raabe D 2021 *Acta Materialia* **204** 116505
[10] Britton T B and Wilkinson A J 2012 *Ultramicroscopy* **114** 82-95